

Collateral ventilation by diffusion across the alveolar walls and the exchange of inert gases in the lung

S.C.M. Luijendijk*, W.R. de Vries**, A. Zwart***

Collateral ventilation by diffusion across the alveolar walls and the exchange of inert gases in the lung. S.C.M. Luijendijk, W.R. de Vries, A. Zwart.

ABSTRACT: The underlying hypothesis of this study is that collateral ventilation by diffusion of occluded air spaces in the lungs of patients with chronic obstructive pulmonary disease (COPD) may play a substantial role in the pulmonary gas exchange of these patients. Using a related lung model we have simulated: a) the multiple-breath washout of helium (He) and sulphur hexafluoride (SF₆) from the alveolar space, and b) the washout of inert tracer gases with different blood-gas partition coefficients, range 0.01-330, from mixed venous blood. These computations were carried out for different values of the collateral diffusion capacity (CDC). Next, the results obtained at each individual value of CDC were used to compute the breath number (Ncr) at the crossing-over of the He-SF₆ washout curves and the inert gas shunt fraction Qs/Qc.

Ncr and Qs/Qc range up to about 100 and 0.04, respectively, when CDC_{SF₆} ranges down to about 0.1 ml·min⁻¹·mmHg⁻¹. These ranges for Ncr and Qs/Qc, and the typical finding of relatively large values for Ncr in combination with small values for Qs/Qc, are also reported in the literature for patients with COPD. These agreements thus support our hypothesis. In line with the small values for Qs/Qc, our results further indicate that even large, well-perfused, occluded air spaces in the lung will hardly affect the recovered ventilation/perfusion distribution obtained from inert gas data when CDC_{SF₆} exceeds 0.1 ml·min⁻¹·mmHg⁻¹.
Eur Respir J., 1991, 4, 1228-1236.

The determination of the washout behaviour of tracer gases which are poorly soluble in blood and lung tissue has become an attractive means to study unequal ventilation in mammalian lungs. For that purpose, the most commonly used features of this behaviour are the slope of the alveolar plateau of expirograms obtained from single breath washout manoeuvres and the (multi-) exponential decay of the tracer gas concentration in expired gas from multiple-breath washout experiments. Some years ago, VON NIEDING *et al.* [1] showed that the difference between the (simultaneously measured, normalized) end-tidal concentrations of He and SF₆ changed sign in the course of a multiple-breath washout. This change in sign defines a cross-over point of the corresponding washout curves of He and SF₆. VON NIEDING *et al.* [1] found that, compared to healthy subjects, the breath number at cross-over (Ncr) shifted to a higher value for patients with chronic obstructive pulmonary disease (COPD). Further, Ncr for patients with emphysema appeared to be larger than Ncr for patients with chronic bronchitis [1].

In previous model simulations [2] we have investigated the basic mechanisms underlying the

afore-mentioned shift in Ncr. It was found that a crossing over near the 2nd breath, which is in the range for healthy subjects [1], can be simulated using asymmetric two trumpet models (fig. 1-A). These specific models account for the asymmetric branching pattern of the acinar airways [3, 4]. However, a shift of Ncr into the range for subjects with chronic bronchitis (Ncr=7.4±1.3) and especially into that for subjects with emphysema (Ncr=62±13) [1] could only be simulated using models with reduced airway cross-sections in a part of the model (fig. 1-B) [2]. These specific models account for the limited mixing of tidal gas with residual gas in partially obstructed air spaces within the lung. The results of these model simulations showed that the presence of convective flow to partially obstructed air spaces interferes with a delayed crossing over [2]. This is due to the fact that the shift in Ncr is related to the difference in diffusive gas transport between He and SF₆, and the corresponding relative difference in overall gas transport between these gases is strongly reduced even by a small convective flow to the partially obstructed air spaces. In this connection we now think that the occurrence of a delayed crossing-over of the

* Dept of Pulmonology, University Hospital Maastricht, State University of Limburg, P.O. Box 5800, 6202 AZ Maastricht, The Netherlands.

** Dept of Medical Physiology, State University of Utrecht, Vondellaan 24, 3521 GG Utrecht, The Netherlands.

*** TNO-CIVO, Toxicology and Nutrition Institute, Utrechtseweg 48, 3704 HE Zeist, The Netherlands.

Keywords: Blood solubility; chronic obstructive pulmonary disease; shunt perfusion; ventilation-perfusion.

Received: December 28, 1989; accepted for publication June 11, 1991.

He-SF₆ end-tidal clearance curves may be primarily related to collateral, diffusive gas exchange between trapped and non-trapped gas in the lung.

In this study, we have modelled collateral ventilation of occluded air spaces by diffusion across lung tissue. Results will be presented relating the value of NCR to both the volume of trapped gas (TGV) and the collateral diffusion capacity (CDC) of the tissue-interfaces between trapped and non-trapped residual gas. In addition, the results of the transpulmonary exchange of inert tracer gases will be presented to assess the influence of CDC on the ventilation-perfusion distribution when determined with the multiple inert gas elimination technique [5].

supplemented with compartments for lung tissue and lung perfusion. These added compartments form the origin of the main differences between the two applied computer programs, and in a sense the one program was an extension of the other. Therefore, we need to discuss only the basic properties of the numerical procedure used for the computation of transpulmonary gas exchange.

The geometry of the airway model was based on morphological data published by WEIBEL [6], HANSEN and AMPAYA [3] and HANSEN *et al.* [4]. The model consisted of a rigid and an expansile part. The rigid part represented the larger airways (mouth up to and including the 10th airway generation). The remaining

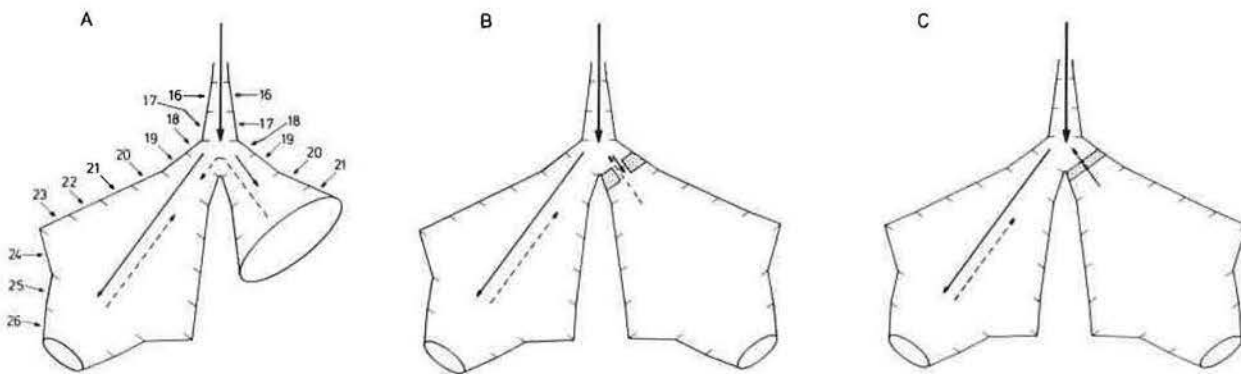


Fig. 1. - Schematic representation of airway models used in computations of pulmonary gas exchange. Panel A: Axis-asymmetric model representing the asymmetric branching pattern of acinar airways. Panel B: Cross-section asymmetric model representing airway narrowing in a part of the lung. Panel C: Cross-section asymmetric model representing totally occluded airways in a part of the lung. Full arrows represent the distribution of airflow within each model during inspiration. Dashed arrows represent direction of gas transport by diffusion in the gas phase during inspiration, and dotted arrow indicates gas transport by collateral diffusion from occluded to non-occluded part of the model.

Materials and methods

Lung model and numerical procedure

The calculations were carried out with two different computer programs, one for the computation of NCR of He-SF₆ washout curves and one for the computation of the transpulmonary exchange of inert tracer gases. The two computer programs were based on the same airway model which is schematically represented in figure 1-C. One of the two cones shown in this figure is closed at its inlet by a barrier which is assumed to allow diffusive gas exchange between trapped gas beyond the barrier and non-trapped gas in the remaining part of the airway model. This model closely resembles the model with the partial airway occlusion (fig. 1-B) which was used in a previous work [2] to simulate the phenomenon of the cross-over. In fact, the two models (figs. 1-B and C) have identical gas exchange properties when no convective flow is allowed to the obstructed part of the model shown in figure 1-B as in that case only diffusive gas exchange across the partial obstruction will remain. For modelling transpulmonary gas exchange, the airway model (fig. 1-C) was

expansile part represented the region where gas exchange takes place between the dissolved tracer gas in blood and lung tissue and tracer gas in the airways. The oscillatory nature of breathing causes within-breath partial pressure oscillations of the tracer gases in the airways and, consequently, also in superficial lung tissue and capillary blood. The within-breath variations in the amount of tracer gas dissolved in this lung tissue and capillary blood interferes with transpulmonary gas exchange mainly for highly soluble tracer gases [7]. The total volume of superficial lung tissue and capillary blood will amount to about 200 ml [6]. In our computations, tissue/gas and blood/gas partition coefficients were assumed to be equal. Therefore, the buffering capacity of superficial lung tissue and capillary blood was equivalent to that of an air space with a volume equal to 200 ml times the blood/gas partition coefficient (λ) of the tracer gas. This virtual volume was added in a proportional way to the geometrical volume of the expansile part of the airway model without changing the cross sections and the lengths of the airways in the model.

To enable the use of difference equations, the airway model was subdivided into 341 serial airway

compartments [8]. The gas transport in the larger airways was calculated on the basis of a dominating convective transport; a slight axial, convective mixing between successive compartments was routinely taken into account. However, the contribution of this mixing to alveolar ventilation is very small [2]. In the expansile part of the model, gas transfer between successive compartments (Δn_1) during the time interval ($t, t+\Delta t$) was calculated by means of the following mass transport equation that includes Fick's diffusion equation and a term that accounts for the convective transport [8]:

$$\Delta n_1 = -D \cdot S \cdot (\Delta C / \Delta l) \cdot \Delta t + \dot{V} \cdot C \cdot \Delta t \quad (1)$$

In addition, gas transport between capillary blood and compartmental gas was calculated from:

$$\Delta n_2 = \dot{q} \cdot (C\bar{v} - \lambda C) \cdot \Delta t \quad (2)$$

where D = molecular diffusion coefficient of the tracer gas; S = cross-section of imaginary dividing surface between successive compartments; C = concentration of tracer gas in the gas phase; ΔC = concentration difference between successive compartments; Δl = axial length of the compartment; \dot{V} = local flow of the gas mixture; \dot{q} = compartmental capillary perfusion and $C\bar{v}$ = concentration of tracer gas in mixed venous blood.

The net gas transfer, Δn , to an expansile compartment during the time interval ($t, t+\Delta t$) was obtained by summation of the results of equation 1 for both imaginary surfaces belonging to this compartment and the result of equation 2. The concentration of the gas at time $t+\Delta t$, $C(t+\Delta t)$, was then computed from:

$$C(t+\Delta t) = [V(t) \cdot C(t) + \Delta n] / V(t+\Delta t) \quad (3)$$

where $V(t)$ is the volume of the compartment (gas volume + virtual volume) at time t . Other features of the calculations were: use of discrete time periods Δt less than $10^{-2} \text{ cm}^2/D$; adjustment of the dimensions of the expansile part of the airway model corresponding to actual lung volume after each time period Δt ; instantaneous, radial partial pressure equilibrium within the compartment as well as between the gaseous phase and the dissolved phase of the tracer gas in lung tissue and capillary blood; synchronous inflation and deflation throughout the non-occluded, expansile part of the airway model; non-pulsatile perfusion; homogeneous perfusion to volume (\dot{Q}_P/V) distribution in the expansile part of the lung model.

The computed results of transpulmonary gas exchange were expressed in terms of excretion ($E = P\bar{E}/P\bar{v}$) and retention ($R = P_a/P\bar{v}$), where $P\bar{E}$, P_a and $P\bar{v}$ represent the partial pressures of the tracer gas in mixed expired gas, arterial blood and mixed venous blood, respectively [5], and each computation was continued until breath-to-breath constant values were obtained for E and R . For further details of the computational procedure we refer to previous publications [2, 7, 8].

Materials

Before each calculation, the dimensions of the applied airway model were scaled up to a preselected total lung capacity (TLC) of 6.5 l yielding an anatomical dead space of 140 ml. Functional residual capacity (FRC) was taken equal to 70% TLC, which accounts for the increase in FRC in patients with COPD as compared to healthy subjects, where $FRC \approx 50\%$ TLC [9]. The following quantities define the applied breathing pattern: tidal volume 700 ml, inspiratory duration 1.5 s and expiratory duration 2.5 s [10]. As a result, minute ventilation (\dot{V}_E) is equal to 10.5 l·min⁻¹. The flow was taken to be constant during both inspiration and expiration without smooth transitions between these two phases. Pulmonary perfusion (\dot{Q}_P) was taken equal to 6 l·min⁻¹. As extrapulmonary shunt has not been considered, \dot{Q}_P was equal to cardiac output (\dot{Q}_C). To the best of our knowledge, diffusion capacities of He and SF₆ for lung tissue are not reported in the literature. Therefore, the ratio of the CDC's for He and SF₆ was estimated from:

$$CDC_{He}/CDC_{SF_6} = (\lambda_{He}/\lambda_{SF_6}) \cdot (M_{SF_6}/M_{He})^{0.5} \quad (4)$$

where λ = tissue/gas partition coefficient and M = molecular weight. Actually, this equation cannot be applied to media consisting of several compounds with widely varying solubility coefficients for the tracer gases. For lung tissue this especially holds true for SF₆, because the oil/water partition coefficient for SF₆ is equal to 66 [11]. This means that small amounts of lipids will contribute considerably to the solubility of SF₆ in lung tissue [12]. However, small amounts of lipids will hardly affect the CDC for SF₆ in lung tissue because the diffusive tissue-barrier mainly consists of water. This stipulates the uncertainty in the estimation of CDC_{He}/CDC_{SF_6} from equation 4. On the basis of the above reasoning we have applied the ratio of the solubility coefficients for He and SF₆ determined by CANDER [13] in washed lung tissue homogenates in which most of the lipids are assumed to be removed [12], namely $\lambda_{He}/\lambda_{SF_6} = 1.353$. In that case, $CDC_{He}/CDC_{SF_6} = 8.2$ (Eqn. 4). Collateral diffusion takes place partly in the gaseous phase. In alveolar gas, the ratio of the diffusion capacities for He and SF₆ (=7.2) is equal to the ratio of their molecular diffusion coefficients which are 0.725 and 0.101 cm²·s⁻¹, respectively [14] i.e., the ratio of the diffusion capacities for He and SF₆ appears to be about the same for lung tissue and alveolar gas. For the calculation of the He-SF₆ washout curves we have used the ratio: $CDC_{He}/CDC_{SF_6} = 7.2$.

Transport of gases by collateral diffusion means that the gases cross the septa between adjacent acinar air spaces. These septa are mainly formed by the alveolo-capillary membranes i.e., the outer walls on both sides of the septa are formed by the alveolar membranes, and the capillaries are in between. Experimental data for CDC_{SF_6} are not known to us, however, the maximum value for CDC_{SF_6} may be estimated from the diffusion capacity of the alveolo-capillary membrane (D_M) for CO. CO is about 2.5 times more soluble in

lung tissue than SF₆ [13, 15], and the molecular mass of SF₆ is about 5 times that of CO. DM_{CO} is about 57 ml·min⁻¹·mmHg⁻¹ [16], therefore, using equation 4, DM_{SF₆} may be about 10 ml·min⁻¹·mmHg⁻¹. In estimating maximum CDC_{SF₆}, we have to take into account that the diffusive path length for SF₆ in the afore described interface (tissue-blood-tissue) between adjacent acinar air spaces is twice as long as that for CO up to the haemoglobin in the capillary blood and that the total surface of the tissue-blood-tissue interface between occluded and non-occluded parts of the lung is at the most one-half of the total surface of the alveolo-capillary membranes. Therefore, maximum CDC_{SF₆} may be about 2.5 ml·min⁻¹·mmHg⁻¹. However, real values for CDC_{SF₆} will be considerably smaller because the surface of the septa between adjacent acinar air spaces that is actually involved in collateral diffusion in the diseased lung will be much smaller than one half of the total surface of the alveolo-capillary membranes. Due to the uncertainty concerning the actual value of CDC_{SF₆} in COPD patients we have chosen different values for CDC_{SF₆} in the computations which cover a wide range namely CDC_{SF₆}=7.87, 0.787, 0.262, 0.0787, and 0.0262 ml·min⁻¹·mmHg⁻¹, respectively. In accordance with the above discussion most of these values are less than 2.5 ml·min⁻¹·mmHg⁻¹.

Three realistic values were used for TGV/FRC, 0.158, 0.286 and 0.472, where TGV is the volume of trapped gas in the occluded part of the airway model [9]. The Q_P/V distribution in the expansile part of our lung model was chosen to be homogeneous. As a consequence, for the largest value of TGV/FRC the volume and perfusion of the occluded part of the model were about 50% FRC and 50% Q_P, respectively. These percentages compare well with the results obtained by BRISCOE *et al.* [17] and FINLEY [18] in patients with severe COPD. These authors found, that the poorly ventilated air spaces in the lungs of those patients constitute on average two-thirds of FRC while receiving one half of Q_c.

The E-R values were computed for 12 hypothetical tracer gases with different λ: λ=0.01, 0.2, 0.4, 0.7, 1.0, 1.5, 2.5, 5.0, 10.0, 30.0, 110.0 and 330.0, respectively, and a single D-value (0.15 cm²·s⁻¹) was used for all these gases. The selected D and λ-values are representative for the tracer gases used in the multiple inert gas elimination technique [5]. Further, CDC of the tracer gases was assumed to be proportional to λ. The partition coefficients of SF₆ for human blood and lung tissue are approximately equal to 0.0067 [13, 19-21], therefore, CDC for λ=0.0067 was chosen to be equal to CDC_{SF₆}. The E-R values were computed for the same series of values for CDC_{SF₆} and TGV/FRC as used for the computation of Ncr.

Results

He-SF₆ cross-over

In figure 2, three pairs of washout curves for He and SF₆ are displayed on a semi-logarithmic scale. Each pair shows a crossing-over of the two washout curves.

These examples thus demonstrate that the phenomenon of the He-SF₆ cross-over can be simulated with lung models which account for collateral ventilation by diffusion of completely occluded air spaces. In table 1, the breath numbers and concentrations of He and SF₆ at cross-over are given for different combinations of the values of CDC_{SF₆} and TGV/FRC. The results show that Ncr increases a) with increasing TGV/FRC and b) with decreasing CDC_{SF₆}. For the determination of Ncr the end-tidal concentrations of He and SF₆ during the washout are normalized relative to their values at the beginning of the washout. Accordingly, the concentrations of He and SF₆ at cross-over are expressed as a percentage of their initial values. The results show that this percentage tends to decrease with increasing value of Ncr.

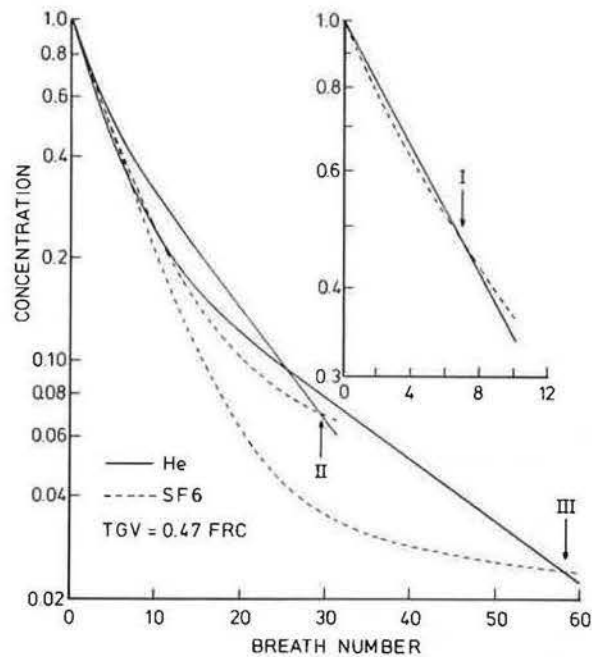


Fig. 2. - Simulated cross-over of He and SF₆ washout curves for different values of collateral diffusion capacity for SF₆ (CDC_{SF₆}). The cross-overs I, II and III refer to CDC_{SF₆}=7.87, 0.787 and 0.262 ml·min⁻¹·mmHg⁻¹, respectively. —: He; - - -: SF₆.

Table 1. - Breath number and concentration of tracer gases at cross-over for different values of CDC_{SF₆} and TGV/FRC

TGV/FRC	CDC _{SF₆}				
	7.87	0.787	0.262	0.0787	0.0262
0.158	no	no	22	66	164
			10.3%	0.8%	0.2%
0.286	4	22	44	104	278
	65.0%	10.7%	2.6%	0.7%	0.2%
0.472	7	30	59	156	438
	47.2%	6.8%	2.4%	0.8%	0.3%

%: concentration of tracer gases as % of concentration at beginning of washout. CDC_{SF₆}: collateral diffusion capacity for SF₆ ml·min⁻¹·mmHg⁻¹; TGV: trapped gas volume; FRC: functional residual capacity.

Excretion and retention

The computed excretion and retention data are represented as E-R diagrams in figure 3. Each curve is based on twelve (E,R) data points, as shown by the curve with dots. The dots correspond to the twelve selected λ -values, respectively, and the first dot on the left hand side of the curve corresponds to $\lambda=0.01$ and the last dot on the right hand side of the curve corresponds to $\lambda=330.0$. In a similar way, λ increases along the other curves shown in figure 3. Further, (E,R) data points on the different curves that correspond to the same λ -value are located on a straight line through the point (E=0, R=1) [7, 22]. This is shown for $\lambda=0.7$. The curve with dots was obtained from calculations with a symmetrically branching airway model without occlusions, *i.e.* the model shown in figure 1-C without occlusion. The remaining four curves were obtained from calculations with the model with an occluded part (TGV/FRC=0.472), and from left to right these curves correspond to $CDC_{SF_6}=0.262$, 0.0787, 0.0262 and 0 $\text{ml}\cdot\text{min}^{-1}\cdot\text{mmHg}^{-1}$, respectively. $CDC_{SF_6}=0$ means that the occluded part of the model was not ventilated at all. Evidently, the curve with dots (model without occlusions) together with the curve that corresponds to $CDC_{SF_6}=0$ constitute the boundaries between which the curves are located for $CDC_{SF_6}>0$.

Figure 3 refers to the largest value of TGV/FRC used in this study, and concerning the other values of TGV/FRC only the boundaries of the E-R curves are displayed in figure 4. The dotted curve in figure 4 is identical to the dotted curve in figure 3 and represents the E-R diagram of the symmetric airway model without occlusions. The remaining three curves are thus obtained with $CDC_{SF_6}=0$ and from left to right they refer to TGV/FRC=0.158, 0.286 and 0.472, respectively.

All curves in figures 3 and 4 show a similar shape. The values of R at the intercepts of the curves with the R-axis reflect the different inert gas shunt fractions (\dot{Q}_s/\dot{Q}_c) [22]. Table 2 shows that \dot{Q}_s/\dot{Q}_c increases with decreasing CDC_{SF_6} and with increasing TGV/FRC. In the gas exchanging part of our model, compartmental perfusion is proportional to compartmental gas volume at FRC (Methods). One might think, therefore, that \dot{Q}_s/\dot{Q}_c for $CDC_{SF_6}=0$ should be equal to TGV/FRC. However, FRC also includes the volume of the larger airways which are not perfused, and this explains why \dot{Q}_s/\dot{Q}_c for $CDC_{SF_6}=0$ is slightly larger than TGV/FRC (table 2).

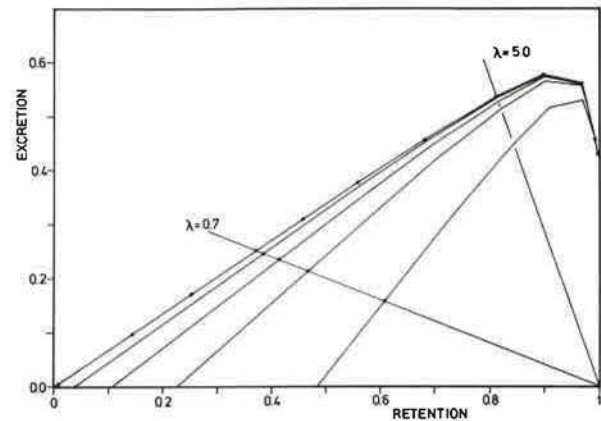


Fig. 3. - Simulated excretion-retention (E-R) diagrams for different values of collateral diffusion capacity for SF_6 (CDC_{SF_6}). Each diagram is composed of 12 (E,R) data points which correspond to different λ -values ranging from 0.01 up to 330.0. The curve with dots was obtained from calculations with a symmetric airway model without occlusions and without collateral diffusion. From left to right the curves correspond to $CDC_{SF_6}=0.262$, 0.0787, 0.0262 and 0 $\text{ml}\cdot\text{min}^{-1}\cdot\text{mmHg}^{-1}$, respectively. $CDC_{SF_6}=0$ implies a real intrapulmonary shunt. CDC was assumed to be proportional to λ , and CDC for $\lambda=0.067$ was chosen to be equal to CDC_{SF_6} (see Materials). Trapped gas volume/functional residual capacity (TGV/FRC)=0.472.

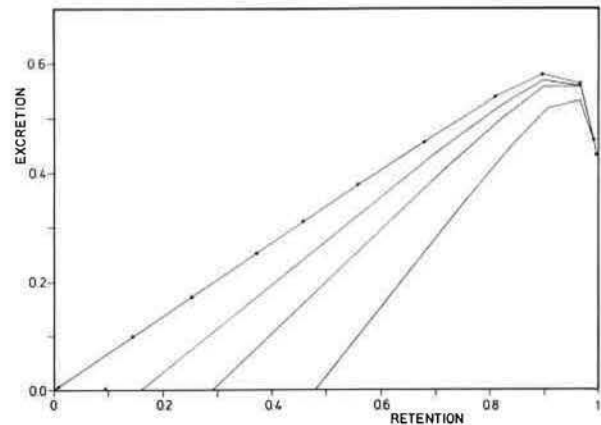


Fig. 4. - Simulated excretion-retention (E-R) diagrams for different values of trapped gas volume/functional residual capacity (TGV/FRC). The curve with dots is identical to the curve with dots in figure 3. From left to right the curves correspond to TGV/FRC=0.158, 0.286 and 0.472, respectively, and these curves were computed with collateral diffusion capacity for SF_6 (CDC_{SF_6})=0.

Table 2. - Inert gas shunt fractions for different values of CDC_{SF_6} and TGV/FRC

TGV/FRC	CDC_{SF_6}					
	7.87	0.787	0.262	0.0787	0.0262	0
0.158	0.000	0.002	0.004	0.014	0.038	0.161
0.286	0.001	0.005	0.015	0.043	0.102	0.292
0.472	0.001	0.014	0.039	0.108	0.224	0.484

For abbreviations see legend to table 1. CDC_{SF_6} $\text{ml}\cdot\text{min}^{-1}\cdot\text{mmHg}^{-1}$.

Discussion

Choice of the applied model

It is obvious, that models based on ventilation by convection only cannot account for the cross-over of the He-SF₆ washout curves or any difference in behaviour between these two gases during washout. In our previous study we have simulated this cross-over phenomenon with a model that included a poorly ventilated compartment which was ventilated by convection and diffusion in parallel (fig. 1-B) [2]. The results showed that large values for NCR can only be obtained when ventilation by convection is nil or nearly so. Thus, we arrived at the conclusion that the late cross-over of the He-SF₆ washout curves, as seen in patients with emphysema [1], might be related to the washout of these gases from occluded air spaces in the lung by diffusion *via* collateral pathways.

According to HILPERT [23] gas transfer across the boundaries between occluded and non-occluded parts of the lung may result from convection and diffusion, but he calculated that transfer by convection through the pores of Kohn would be much more important than transfer by diffusion across the tissue boundaries. Gas transfer by diffusion, however, may also take place *via* the pores of Kohn together with gas transfer by convection. For gas transfer by diffusion to be comparable with that by convection, the velocity of alveolar gas in the pores of Kohn should be about 6 mm·s⁻¹, which we learnt from our previous studies on convective-diffusive inter-dependence of gas mixing in the alveolar space [8]. For the computation of the flow through the pores of Kohn, HILPERT [23] made use of equations that apply to flow through orifices. Using the same equations it can be shown that the afore-mentioned velocity of alveolar gas in the pores of Kohn corresponds to a pressure difference across the alveolar wall of about 40 μPa. Hence, even the slightest pressure difference would be sufficient to abolish the contribution of diffusion to gas transfer *via* open pores of Kohn. This result together with the result of the computations of Hilpert lead to the conclusion that the contribution of diffusion to collateral ventilation is negligible as compared to the contribution of convection. This would mean that the model used for the present study is invalid. It should be noted, however, that the validity of the above conclusion fully depends on the validity of the assumption that pores of Kohn are open air passages. This is not certain as these small pores may be filled with extracellular fluid from the alveolar surface. MARTIN [24] pointed out that those pores would require very large pressure differences between their ends far exceeding the pressure differences that occur in the lung to be opened again. Thus, pores of Kohn filled with fluid may represent the normal situation. It is known from anaesthesiology that it can be dangerous to use N₂O in patients with severe COPD, because application of this anaesthetic gas causes the pulmonary blebs to enlarge with concomitant damage of lung tissue and pneumothorax [25, 26]. In this respect, the

pulmonary blebs behave in the same way as other internal gas spaces enclosed in organs with compliant walls (colon, small intestine, stomach) [25]. The distention of these closed gas spaces is due to the fact that during the early stage of anaesthesia the influx of the more soluble gas N₂O is larger than the efflux of N₂. Use of high concentrations of N₂O in inspired gas during anaesthesia amplifies the condition [25]. Obviously, the distention of the pulmonary blebs would not occur if pressure equilibration of occluded lung units *via* collateral pathways took only a few seconds as has been observed in dogs [27]. In healthy human lungs, however, this equilibration is much slower, and in patients with COPD it is very slow [27]. These data and the experience of anaesthetists with the application of N₂O anaesthesia in patients with COPD, support the underlying assumptions of our model that parts of the lungs of COPD patients are essentially occluded for convective gas transport and that those areas are ventilated *via* the remaining collateral pathway of diffusion through the tissues of the alveolar walls.

Cross-over of He and SF₆ washout curves

According to the observations of VON NIEDING *et al.* [1], NCR ranges from about 5 up to about 90. The results for NCR obtained with the model with collateral ventilation by diffusion thus cover the whole range of NCR values observed in patients with COPD. The model results, however, also show values which substantially exceed the range of measured values for NCR. Apparently, the very large values for NCR (>150) obtained in particular for CDCSF₆=0.0262 are not observed in practice. This discrepancy may be due to the selection of CDCSF₆ values, *i.e.* the smallest value of CDCSF₆ (=0.0262) used in our computations may be too small so that it underestimates the overall CDCSF₆ between occluded and non-occluded parts of the lung for the given values of TGV/FRC.

VON NIEDING *et al.* [1] did not report the concentrations of He and SF₆ at the observed cross-over points. Illustrations of He and SF₆ washout curves in their paper, suggest that, in general, the measured concentration of these tracer gases at cross-over decreased with increasing NCR. The same relationship was obtained from our model computations. This is a trivial relationship when groups of subjects are compared with large differences in NCR like healthy subjects and patients with emphysema. It is likely, however, that an inverse relationship between the concentration of He and SF₆ at cross-over and NCR will not be found in a group of subjects with approximately the same NCR values, *e.g.* in patients with chronic bronchitis, as NCR may also depend on parameters such as respiratory rate and FRC/TLC [1].

Excretion-retention data

The shape of the curves in figure 3 is convex for those parts which correspond to λ-values larger than

about 5.0. This shape is related to the tidal nature of breathing and the within-breath uptake and release of tracer gases by superficial airway tissue. This phenomenon has been extensively discussed elsewhere [7]. Gas transport by collateral diffusion augments the alveolar partial pressure (P_A) of the tracer gases in the non-occluded part of the lung model. For tracer gases with very large λ -values, however, P_A is close to P_V , and, consequently, for these gases collateral diffusion will hardly affect P_A . This explains that the same excretion and retention data are obtained for $\lambda=110$ irrespective of the value of CDC_{SF_6} , and likewise for $\lambda=330$.

For $\lambda < 5$ the E-R curves are almost straight lines. E-R data which form a straight line in the E-R diagram can be described by a classical lung model consisting of three parallel compartments namely a shunt compartment, a dead space compartment and a compartment that is both ventilated and perfused [22]. Concerning our E-R data this means that the ventilation-perfusion ratio (\dot{V}_A/\dot{Q}) of the latter compartment is equal to the slope of the E-R line for $\lambda < 5$ times \dot{V}_E/\dot{Q}_C .

For small values of CDC_{SF_6} ($\neq 0$) the occluded part of our model is poorly ventilated, whereas its perfusion is normal. As mentioned above, in terms of the classical lung model a shunt fraction is obtained, whereas a compartment with a small \dot{V}_A/\dot{Q} value ($\neq 0$) will not be recovered. Apparently, this shunt fraction accounts for the impaired gas transport of the occluded part of our model. Accordingly, \dot{Q}_S/\dot{Q}_C increases with decreasing CDC_{SF_6} (table 2), where $\dot{Q}_S/\dot{Q}_C = \dot{Q}_{P,occl}/\dot{Q}_P$ for $CDC_{SF_6} = 0$. $\dot{Q}_{P,occl}$ is the perfusion of the occluded part of the model. An important consequence of the data shown in table 2 is that in diffuse airway obstruction, a large number of well-perfused, occluded parts of the lung may result in only a small inert gas shunt fraction due to the ventilation of these parts by collateral gas transport by diffusion. This point is further discussed when the results of our model simulations are compared to the results for NCR and \dot{Q}_S/\dot{Q}_C found in patients with COPD.

The presentation of the E-R curves in figure 4, as well as the presentation of the results for \dot{Q}_S/\dot{Q}_C in table 2, suggest that the E-R data also depend on the volume of trapped gas. This, however, is not true. The diffusive transport of the gases within the occluded part of our model is very efficient as compared to the diffusive transport between the occluded and non-occluded parts of the model. Therefore, the simulated E-R data in this study will hardly depend on the actual volume of trapped gas. Thus, what remains is the dependence of E and R on both CDC_{SF_6} and $\dot{Q}_{P,occl}$. The applied modelling of perfusion, where $\dot{Q}_{P,occl}$ is proportional to TGV, explains why different curves are obtained in figure 4 for different values of TGV/FRC. For the same reason the increase in \dot{Q}_S/\dot{Q}_C with increasing TGV/FRC (fig. 4, table 2) is due to the increase in $\dot{Q}_{P,occl}/\dot{Q}_P$. This direct relationship between \dot{Q}_S/\dot{Q}_C and $\dot{Q}_{P,occl}/\dot{Q}_P$ clearly demonstrates the obvious result that the negative effect of occluded lung regions on transpulmonary gas exchange is diminished when

$\dot{Q}_{P,occl}$ is reduced. The following preliminary conclusions can now be drawn: NCR depends on CDC_{SF_6} and TGV, and \dot{Q}_S/\dot{Q}_C depends on CDC_{SF_6} and $\dot{Q}_{P,occl}/\dot{Q}_P$. From a purely theoretical point of view this means that there is no unique relationship between NCR and \dot{Q}_S/\dot{Q}_C , this is also shown by the data given in tables 1 and 2. Thus, any combination of measured values for NCR and \dot{Q}_S/\dot{Q}_C can be simulated by selecting appropriate values for TGV, CDC_{SF_6} and $\dot{Q}_{P,occl}/\dot{Q}_P$. For example a combination of values for TGV and CDC_{SF_6} may be first selected to meet the value of NCR. Next, at the already selected value for CDC_{SF_6} , a value for $\dot{Q}_{P,occl}/\dot{Q}_P$ can be selected so that this combination of values meets the value of \dot{Q}_S/\dot{Q}_C . Therefore, collateral diffusion between occluded and non-occluded parts of the lung could account for any combination of values for NCR and \dot{Q}_S/\dot{Q}_C that may be found in patients with COPD.

How do our model predictions compare with experimental data?

We already mentioned that our simulated values for NCR (table 1) cover the whole range of measured values for NCR in a group of patients with different types of COPD [11].

BRISCOE *et al.* [17] and FINLEY [18] determined indices of ventilation-perfusion inhomogeneity in patients with severe emphysema. They measured simultaneously the changes in the saturation [17] or the partial pressure [18] of oxygen in arterial blood and the multiple-breath washout of N_2 during breathing 100% O_2 . They further applied a two compartment analysis of their data. They found that on the average the poorly ventilated compartment constituted 67% FRC and was ventilated by 12% V_A which corresponded to about $600 \text{ ml}\cdot\text{min}^{-1}$. In our model the same alveolar ventilation for N_2 of the occluded part will be obtained when $CDC_{N_2} = 0.652 \text{ ml}\cdot\text{min}^{-1}\cdot\text{mmHg}^{-1}$ as $600 = 0.652 \times 760 \times (310/273) \times (760/713)$ where the last two terms refer to the conversion from STPD to BTPS. Taking into account the difference in λ and molecular weight between N_2 and SF_6 , this value for CDC_{N_2} corresponds to $CDC_{SF_6} = 0.14$. Application of TGV/FRC = 0.67 and $CDC_{SF_6} = 0.14$ to our model will result in a value for NCR > 60 (table 1) which is compatible with the range of NCR values observed in patients with emphysema [1]. Thus, on the basis of our model and its underlying assumptions the experimental findings reported for NCR [1] and for the volume and ventilation of the poorly ventilated alveolar space in patients with emphysema [17, 18] are mutually consistent.

WAGNER *et al.* [28] determined the values for \dot{Q}_S/\dot{Q}_C with the multiple inert gas elimination technique in a group of 23 patients with COPD. The values for \dot{Q}_S/\dot{Q}_C ranged from 0.0 up to 22.2%. Large values for \dot{Q}_S/\dot{Q}_C (>10%) were obtained in only 2 patients, whereas in the remaining 21 patients \dot{Q}_S/\dot{Q}_C ranged from 0.0 up to 4.4% with a mean value of 0.7%. Hence, in general, only small values for \dot{Q}_S/\dot{Q}_C have been found. Similarly,

small values (<0.044) are shown in table 2 for the results of \dot{Q}_s/\dot{Q}_c obtained from the combinations of TGV/FRC and CDC_{SF_6} which correspond to realistic NCR values ($5 < NCR < 90$) for COPD patients (table 1). This also means that consistent model results were obtained for Ncr and \dot{Q}_s/\dot{Q}_c , and these results further indicate that for realistic values of NCR and \dot{Q}_s/\dot{Q}_c , CDC_{SF_6} should be larger than about $0.08 \text{ ml}\cdot\text{min}^{-1}\cdot\text{mmHg}^{-1}$ (tables 1 and 2). This value corresponds to 3.2% of maximum CDC_{SF_6} which was assumed to be about $2.5 \text{ ml}\cdot\text{min}^{-1}\cdot\text{mmHg}^{-1}$ (see Materials).

As already mentioned, \dot{Q}_s/\dot{Q}_c is equal to the value of R at the intercept of the E-R curve with the R-axis. As a consequence, the E-R curves with $\dot{Q}_s/\dot{Q}_c < 0.044$ are very close together in the E-R diagram as may be inferred from the curves shown in figure 3. On the basis of the small values for \dot{Q}_s/\dot{Q}_c found in patients with COPD this finding of our model simulations suggests that the impact on the recovered \dot{V}_A/\dot{Q} -distribution of lung regions that are ventilated by collateral diffusion only will be small in these patients. In other cases, however, collateral ventilation by diffusion may well affect the recovered \dot{V}_A/\dot{Q} -distribution, e.g. when parts of the lung that are poorly ventilated by tidal gas in the normal way are, in addition, ventilated by collateral diffusion. This particular case will be discussed below.

It is remarkable that in many of the COPD patients studied by WAGNER *et al.* [28] the recovered \dot{V}_A/\dot{Q} distribution did not show a low \dot{V}_A/\dot{Q} mode. This is an intriguing result as COPD patients in particular will show lung regions that are poorly ventilated. However, on the basis of the results of this model study the following may be considered. The occluded part of our model is ventilated only by collateral diffusion, whereas its perfusion is normal, nevertheless, none of the simulated E-R data sets give rise to a low \dot{V}_A/\dot{Q} compartment with $\dot{V}_A/\dot{Q} \neq 0$ because each E-R data set constitutes a straight line in the E-R diagram for $\lambda < 5$ [22]. This behaviour of the E-R data sets must be ascribed to the fact that CDC of the tracer gases is chosen to be proportional to λ , and from a physical point of view this a reasonable assumption. As a consequence, the ventilation of the occluded part of our lung model depends on λ . Therefore, the excretion-retention behaviour of this occluded part is fundamentally different from that of a lung compartment that is directly ventilated by tidal gas because in that case ventilation is independent of λ . In the real lung, the E-R behaviour of a lung compartment that is poorly ventilated by tidal gas may be substantially affected by collateral diffusion, i.e. for such a compartment the contribution of collateral diffusion to compartmental gas exchange may become important, and the aforesaid E-R behaviour that corresponds to collateral ventilation by diffusion will counteract the occurrence of low \dot{V}_A/\dot{Q} modes in the recovered \dot{V}_A/\dot{Q} distribution. On the basis of the delayed cross-over of He-SF₆ washout curves in COPD patients we think that collateral ventilation by diffusion plays an important role in the gas exchange of poorly ventilated lung regions. Thus,

the absence of low \dot{V}_A/\dot{Q} modes in about half of the recovered \dot{V}_A/\dot{Q} distributions of the COPD patients studied by WAGNER *et al.* [28] may mean that according to the usual interpretation of E-R data these patients had no lung compartments with low \dot{V}_A/\dot{Q} , or that the ventilation of these lung compartments was mainly the result of collateral diffusion. The former possibility, however, would be in conflict with the observations of BRISCOE *et al.* [17] and FINLEY [18] who in a comparable group of patients found that the ventilation-perfusion ratio of the poorly ventilated alveolar space was about 0.23.

In summary, the underlying assumptions of this model study are that poorly ventilated lung regions in patients with COPD may, at least in part, be related to completely occluded air spaces, and that ventilation of these air spaces takes place by diffusion of gases across the septa that separate the occluded from the non-occluded air spaces. Accordingly, we have developed a simplified gas exchange model of the lung consisting of two compartments. The one compartment represents all non-occluded air spaces and the other compartment represents all occluded air spaces. The ventilation of the latter compartment has been modelled to reflect collateral ventilation by diffusion across tissue, alveolar walls etc. We have shown that the gas exchange properties of this model agree with those frequently observed in patients with severe COPD, namely a strongly delayed cross-over of the normalized washout curves of He and SF₆, a small inert gas shunt fraction, and the absence of low ventilation/perfusion modes in distributions recovered from excretion and retention data of inert gases. Up to this study these observations could not be described by one single model. Therefore, our findings may have important consequences for respiratory modelling. It is also clear from this paper, however, that further investigations are needed to ascertain whether the underlying assumptions of our model are correct. Therefore, for the time being no final conclusions can be drawn.

References

1. Von Nieding G, Löllgen H, Smidt U, Linde H. - Simultaneous washout of helium and sulphur hexafluoride in healthy subjects and patients with chronic bronchitis, bronchial asthma and emphysema. *Am Rev Respir Dis*, 1977, 116, 649-660.
2. de Vries WR, Luijendijk SCM, Zwart A. - Helium and sulphur hexafluoride washout in asymmetric lung models. *J Appl Physiol: Respirat Environ Exercise Physiol*, 1981, 51, 1122-1130.
3. Hansen JE, Ampaya EP. - Human air space shapes, sizes, areas, and volumes. *J Appl Physiol*, 1975, 38, 990-995.
4. Hansen JE, Ampaya EP, Bryant GH, Navin JJ. - Branching pattern of airways and air spaces of a single human bronchiole. *J Appl Physiol*, 1975, 38, 983-989.
5. Wagner PD, Saltzman HA, West JB. - Measurement of continuous distributions of ventilation-perfusion ratios: theory. *J Appl Physiol*, 1974, 36, 588-599.

6. Weibel ER. - *In: Morphometry of the Human Lung*. Springer-Verlag, Berlin, 1963.
7. Zwart A, Luijendijk SCM, de Vries WR. - Excretion-retention data of steady state gas exchange in tidal breathing. I. Dependency on the blood-gas partition coefficient. *Pflügers Arch*, 1986, 407, 204-210.
8. Luijendijk SCM, Zwart A, de Vries WR, Salet WM. - The sloping alveolar plateau at synchronous ventilation. *Pflügers Arch*, 1980, 384, 267-277.
9. Bedell GN, Marshall R, DuBois AB, Comroe JH Jr. - Plethysmographic determination of the volume of gas trapped in the lungs. *J Clin Invest*, 1956, 35, 664-670.
10. Garrard CS, Lane DJ. - The pattern of breathing in patients with chronic airflow obstruction. *Clin Sci*, 1979, 56, 215-221.
11. Power GG, Stegall H. - Solubility of gases in human red blood cell ghosts. *J Appl Physiol*, 1970, 29, 145-149.
12. Young IH, Wagner PD. - Solubility of inert gases in homogenates of canine lung tissue. *J Appl Physiol: Respirat Environ Exercise Physiol*, 1979, 46, 1207-1210.
13. Cander L. - Solubility of inert gases in human lung tissue. *J Appl Physiol*, 1959, 14, 538-540.
14. Worth H, Piiper J. - Diffusion of helium, carbon monoxide and sulphur hexafluoride in gas mixtures similar to alveolar gas. *Respir Physiol*, 1978, 3, 155-166.
15. Power GG. - Solubility of O₂ and CO in blood and pulmonary and placental tissue. *J Appl Physiol*, 1968, 24, 468-474.
16. Crapo RO, Morris AH, Gardner RM. - Reference values for pulmonary tissue volume, membrane diffusing capacity, and pulmonary capillary blood volume. *Bull Eur Physiopathol Respir*, 1982, 18, 893-899.
17. Briscoe WA, Cree EM, Filler J, Houssay HEJ, Courmand A. - Lung volume, alveolar ventilation and perfusion interrelationships in chronic pulmonary emphysema. *J Appl Physiol*, 1960, 15, 785-795.
18. Finley TN. - The determination of uneven pulmonary blood flow from the arterial oxygen tension during nitrogen washout. *J Clin Invest*, 1961, 40, 1727-1734.
19. Longo LD, Delivoria-Papadopoulos M, Power GG, Hill EP, Forster RE. - Diffusion equilibration of inert gases between maternal and fetal placental capillaries. *Am J Physiol*, 1970, 219, 561-569.
20. Meyer M, Tebbe U, Piiper J. - Solubility of inert gases in dog blood and skeletal muscle. *Pflügers Arch*, 1980, 384, 131-134.
21. Wagner PD, Neumann PF, Laravuso RB. - Simultaneous measurement of eight foreign gases in blood by gas chromatography. *J Appl Physiol*, 1974, 36, 600-605.
22. Zwart A, Luijendijk SCM. - Excretion-retention diagram to evaluate gas exchange properties of vertebrate respiratory systems. *Am J Physiol*, 1982, 243 (Regulatory Integrative Comp Physiol 12), R329-R338.
23. Hilpert P. - He Auswaschung aus stenosierten Lungensegmenten durch kollaterale Ventilation. *Respiration*, 1976, 33, 112-122.
24. Martin HB. - Respiratory bronchioles as the pathway for collateral ventilation. *J Appl Physiol*, 1966, 21, 1443-1447.
25. Eger EI II. - *In: Anesthetic uptake and action*. The Williams & Wilkins Company, Baltimore, USA, 1974, pp. 171-183.
26. Gold MI, Joseph SI. - Bilateral tension pneumothorax following induction of anesthesia in two patients with chronic obstructive airway disease. *Anesthesiology*, 1973, 38, 93-96.
27. Menkes HA, Traystman RJ. - State of the art: collateral ventilation. *Am Rev Respir Dis*, 1977, 116, 287-309.
28. Wagner PD, Dantzker DR, Dueck R, Clausen JL, West JB. - Ventilation-perfusion inequality in chronic obstructive pulmonary disease. *J Clin Invest*, 1977, 59, 203-216.

Ventilation collatérale par diffusion au travers des parois alvéolaires et échanges de gaz inertes au niveau pulmonaire.
S.C.M. Luijendijk, W.R. de Vries, A. Zwart.

RÉSUMÉ: L'hypothèse, à la base de cette étude, est que la ventilation collatérale par diffusion d'espaces aériens clos dans les poumons de patients atteints de maladie pulmonaire obstructive chronique (COPD), pourrait jouer un rôle substantiel dans les échanges gazeux pulmonaires de ces patients. En utilisant un modèle adapté, de poumon nous avons simulé:
a. le wash out d'hélium (He) en respiration multiple et celui d'hexafluorure de soufre (SF₆) à partir de l'espace alvéolaire, et b. le wash out de gaz inertes traceurs avec différents coefficients de séparation sang-gaz, s'étendant de 0.01 à 330, en provenance du sang veineux mêlé.

Ces évaluations computerisées ont été conduites pour différentes valeurs de la capacité de diffusion collatérale (CDC). En outre, les résultats obtenus au niveau de chaque valeur individuelle de CDC ont été utilisés pour computer le nombre respiratoire (Ncr) au croisement des courbes de wash out (He-SF₆) et de la fraction shuntée des gaz inertes (Q_s/Q_c). Ncr et Q_s/Q_c s'étendent d'environ 100 à 0.04 respectivement, lorsque CDC_{SF₆} s'abaisse jusqu'aux environs de 0.1 ml·min⁻¹·mmHg⁻¹. Ces limites pour Ncr et Q_s/Q_c, ainsi que l'observation typique de valeurs relativement élevées pour Ncr en combinaison avec de petites valeurs de Q_s/Q_c, ont également été rapportées dans la littérature pour les patients atteints de COPD. Ces concordances viennent à l'appui de notre hypothèse. Dans la même ligne que les petites valeurs de Q_s/Q_c, nos résultats indiquent par ailleurs que même des espaces aériens clos de grande taille et bien perfusés au niveau du poumon n'affecteront que de manière limite la distribution de la ventilation/perfusion récupérée, que l'on obtient à partir de données des gaz inertes lorsque CDC_{SF₆} dépasse 0.1 ml·min⁻¹·mmHg⁻¹.

Eur Respir J., 1991, 4, 1228-1236.